International Journal of Nanomedicine Dovepress

Open Access Full Text Article ORIGINAL RESEARCH

Long-Circulating Nanoemulsion with Oxygen and Drug Co-Delivery for Potent Photodynamic/Antibiotic Therapy Against Multidrug-Resistant Gram-Negative Bacterial Infection

Xiaolong Li[1], Xinyi Hou[2], Siqin Zhang[1], Jianming Xiong[1], Yuanyuan Li[2,3], Wenjun Miao[1,4]

[1]School of Pharmaceutical Sciences, Nanjing Tech University, Nanjing, 211816, People's Republic of China; [2]School of Pharmacy, Hainan Medical University, Haikou, Hainan, 571199, People's Republic of China; [3]NHC Key Laboratory of Tropical Disease Control, Hainan Medical University, Haikou, Hainan, 571199, People's Republic of China; [4]State Key Laboratory of Materials-Oriented Chemical Engineering, Nanjing Tech University, Nanjing, 211816, People's Republic of China

Correspondence: Yuanyuan Li, School of Pharmacy, Hainan Medical University, Haikou, Hainan, 571199, People's Republic of China, Tel/Fax +86-0898-66968120, Email liyuanyuan@hainmc.edu.cn; Wenjun Miao, School of Pharmaceutical Sciences, Nanjing Tech University, Nanjing, 211816, People's Republic of China, Tel/ Fax +86-25-58139942, Email miaowj@njtech.edu.cn

Purpose: Compared to conventional photodynamic therapy (PDT), oxygen-affording PDT represents a promising strategy for treating multidrug-resistant (MDR) gram-negative bacterial infections due to its enhanced sensitization ability towards bacteria and amplified therapeutic efficacy. Over the last decade, various nanoplatforms for the co-delivery of oxygen and photosensitizers have been developed. However, their application in the treatment of infectious diseases is hampered by their poor stability and easy clearance by the reticuloendothelial system (RES).

Methods: To address these obstacles, we reported an erythrocyte membrane (EM) camouflaged nanoemulsion containing chlorin e6 (Ce6) and perfluorocarbon (FDC), named ECF, showing good colloidal stability and long-circulating potential, making it suitable for fighting against MDR Gram-negative bacterial infections. The nanoemulsion was fabricated and characterized. The oxygen loading and release performance, photodynamic activity, and bactericidal performance of ECF against *Acinetobacter baumannii* (*A. baumannii*) were evaluated. Furthermore, the antiphagocytosis profile was tested in vitro using Raw 264.7 cells. In addition, the pharmacokinetic behavior and therapeutic efficiency of ECF were studied in vivo.

Results: ECF exhibited superior oxygen loading and release behavior, potent photodynamic activity, and negligible toxicity to mammalian cells. Upon light irradiation, the antibacterial rate of preoxygenated-ECF reached 98% at 40 μg mL^{-1} of Ce6 and the bactericidal activity of preoxygenated-ECF and Gen was 3.3 folds higher than that of Gen. Furthermore, ECF could effectively inhibit uptake by phagocytes and circulate in the blood 1.5-fold longer than that of nanoemulsion without EM modification (CF) following intravenous administration. In addition, preoxygenated-ECF combined with antibiotic plus light irradiation showed prominent therapeutic efficacy in treating *A. baumannii*-induced acute peritonitis, accompanied by good biocompatibility in vivo.

Conclusion: Our results provide a novel paradigm for evading immune clearance, prolonging retention time and improving synergetic bactericidal capacity in combination with PDT and antibiotic therapy against planktonic bacteria and gram-negative bacterial infections.

Keywords: Gram-negative bacterial infection, multidrug-resistant, photodynamic therapy, oxygen affording, long circulation

Introduction

Bacterial infectious diseases are emerging as a significant global health concern, causing over 700,000 fatalities annually. As mainstream clinical management, traditional antibiotic therapy has been used for several decades to prevent and combat bacterial infectious diseases.[1–3] Unfortunately, the spread of multidrug-resistant (MDR) bacterial strains, such as *Escherichia coli, Staphylococcus aureus, Pseudomonas aeruginosa,* and *A. baumannii*, etc, has arisen due to the

Received: 16 May 2024
Accepted: 31 October 2024
Published: 21 November 2024

inappropriate and excessive use of antibiotics.[4–6] The effectiveness of conventional antibiotics may be diminished or rendered ineffective against these MDR bacteria because of their precise mutations, the expression of efflux pump, and the up-regulation of defense-associated enzymes, among other factors. It is estimated that the global annual mortality of infectious diseases would be projected at 10 million by 2050 if action is not taken to combat MDR, highlighting the urgent need for the development of alternative treatment strategies for MDR bacterial infections.[7–9] In the battle against MDR bacterial infections, a multitude of antibiotic-independent manners have been explored. Among these, photodynamic therapy (PDT) has garnered tremendous attention, with the merits of high efficiency, minimal invasiveness, and negligible drug resistance.[10–12] PDT utilizes oxygen and photosensitizers (PS) to produce reactive oxygen species (ROS) during appropriate laser irradiation, resulting in the oxidation of biomolecules (lipids, proteins, and cellular DNA) and subsequent bacterial lysis.[10] Nonetheless, previous studies have highlighted a notable distinction in the susceptibility of Gram-positive and Gram-negative bacteria to PDT. PDT demonstrates minimal efficacy in eradicating gram-negative bacteria, as opposed to its effective bactericidal activity against gram-positive bacteria, owing to variations in their respective bacterial structures.[13,14] Thus, it would be of significance and urgency to find a novel strategy for sensitizing gram-negative bacteria towards PDT and enhancing bactericidal efficacy.

As an important factor of PDT, the oxygen concentration has an immediate impact on treatment outcomes. The therapeutic efficacy of PDT can be remarkably improved by continuous oxygen supplement in hypoxic infectious tissue. For instance, Ji's group designed an oxygen-sufficient nanoplatform for potent photodynamic eradication of MDR bacterial biofilm by alleviating the local hypoxic microenvironment.[15] Moreover, we reported a multifunctional perfluorocarbon nanoemulsion to deliver PS and oxygen for combating MDR Gram-negative bacterial infection under laser irradiation. Our findings indicated that the sensitivity of bacteria to PDT could be notably enhanced by supplementing oxygen over treatment course, leading to excellent bactericidal effect.[14] For achieving direct oxygen delivery, hemoglobin and FDC are utilized as conventional nanovehicles.[16] To date, a considerable number of nanosystems incorporating oxygen carriers (such as polymeric micelles and liposomes) have been studied, accompanied by the fast-growing of nanotechnology-based approaches.[17] Nevertheless, these exogenous nanosystems that enter the bloodstream are easily detected as intruders and cleared out from the blood circulation by RES, leading to unsatisfied biocompatibility, retention time in vivo and therapeutic effectiveness. To address this issue, decorating these nanosystems with nature-inspired biomimetic nanomaterials derived from cells, bacteria, and viruses, which can inherit their physiological functions, has become a new research topic in recent years.[18,19]

Among various types of natural biomaterials, surface functionalization using erythrocyte membrane (EM) has been widely adopted because of its unique pharmacokinetic and biodistribution characteristics. Erythrocyte naturally has a long circulation life in the body, lasting for 120 days before immune clearance.[20–22] This is partly because a series of proteins presenting on the erythrocyte membrane surface (C8 binding protein, homologous restriction protein, decay-accelerating factor, membrane cofactor protein, and complement receptor 1) play a role in defending against attacks from complement system.[22,23] Especially, CD47 containing five transmembrane regions and a single Ig-like domain can interact with the NH_2-terminal domain of the signal-regulatory protein alpha (SIRPα) glycoprotein, releasing "don't eat-me" signal to inhibit the clearance of erythrocyte by the immune system.[24,25] We therefore speculated that utilizing EM to cloak and stabilize nanoparticles could endow some advantages, like better biocompatibility, low immune clearance, and prolonged circulation, which favorably alters the distribution and efficacy of the drug in vivo.

In this study, we designed and constructed an EM-modified nanoemulsion (ECF) for co-delivering oxygen and photoactive drugs to fight MDR gram-negative bacterial infections. For fabricating ECF, chlorin e6 (Ce6) and FDC were employed as PS and oxygen cargo, respectively, and then co-loaded into nanoemulsion through hydrophobic interactions. Following that, the nanoemulsion was encapsuled with EM to achieve "stealthy effect" by separating it from the surrounding environment in vivo, which can enhance its stability, antiphagocytosis potential, as well as prolong retention time. We systematically investigated the oxygen delivery behavior, biocompatibility, and photodynamic activity of ECF. Moreover, the bactericidal performance of ECF alone and in combination with gentamicin (Gen) was evaluated against *A. baumannii*. Furthermore, the immune evasion capacity and the pharmacokinetic profile of the proposed nanoemulsion were assessed sequentially and then their bactericidal efficacy and biosafety in an *A. baumannii*–induced mouse peritonitis model (systemic infection) were studied.

Material and Methods

Materials

Ce6 was supplied by Frontier Scientific Inc. (West Logan, UT, USA). FDC, Gen, lecithin and cholesterol were purchased from Aladdin (Shanghai, China). 1.3-diphenylisobenzofuran (DPBF) was obtained from Sigma-Aldrich (St. Louis, USA). Bicinchoninic acid (BCA) test kit was obtained from Beyotime Biotechnology Ltd. (Shanghai, China). Distilled water (DW) used in the experiments was produced using the Milli-Q Direct 16 water purification system (Millipore Corporation, Bedford, MA, United States) with a resistivity higher than 18.2 MΩ cm^{-1}. All other chemicals were obtained from Sinopharm Chemical Reagent Co. (China), unless stated otherwise.

A. baumannii was kindly provided by Dr. Yishan Zheng at The Second Hospital of Nanjing, China. Mouse macrophages (Raw 264.7) and fibroblasts (L929) were obtained from the Institute of Biochemistry and Cell Biology, Chinese Academy of Sciences (Shanghai, China). All reagents and materials used in cell experiments were provided by Gibco BRL Life Technologies.

Isolation of EM

EM was prepared via hypotonic lysis approach following previous literature with slight modifications.[26,27] In brief, fresh blood collected from ICR mice (25–30 g) was stored in a heparin tube and then centrifuged (500 × *g*) for 10 min at 4°C to remove the plasma and buffy coat. After washing with cold PBS and centrifugation several times, the collected erythrocytes were re-suspended in 1/4× phosphate buffer saline (PBS, 150 mm, pH 7.4) at 4°C for 0.5–1 h and then sonicated with a tip for 180 s under an ice bath. The precipitated EM was harvested and stored at − 80°C for further use following the removal of the released hemoglobin through centrifugation. The BCA kit was employed to measure and quantify the protein content of EM based on a standard protocol.[27]

Preparation of ECF Nanoemulsion

Ce6@FDC nanoemulsion (abbreviated as CF) was fabricated by ultrasonic emulsification as described in our previous study.[14] For this purpose, lipids (cholesterol: lecithin=1:2, w/w) and Ce6 were dissolved in chloroform, respectively, and then mixed by stirring at room temperature. Subsequently, the remaining solvent was completely removed by rotary evaporation, and 5 mL of deionized water containing FDC (200 μL) was added to the mixture during sonication. Free Ce6 was removed by gel filtration using a dextran gel column (PD midi Trap G-25, GE Healthcare, United Kingdom) to obtain purified CF nanoemulsion.

For the preparation of EM-coated CF nanoemulsion (abbreviated as ECF), 10 μL EM (1 mg mL^{-1}, in terms of protein) was mixed with CF and sonicated with bath sonicator at a power of 100 W for 30 min. The mixture containing ECF was centrifuged at 3000 × *g* for 30 min and washed with cold PBS for several times, and then the purified ECF was re-suspended in PBS at the desired concentration and stored at 4°C. Meanwhile, Ce6 nanoemulsion (abbreviated as Ce6) was constructed without FDC and the other preparation steps were the same as above. Finally, the oxygenated ECF, designated as ECF+O_2, was obtained by bubbling oxygen for 30 min.

Characterization

The hydrodynamic diameter of ECF and CF was determined by dynamic light scattering (DLS) with a 10 mW He-Ne laser at 25°C, and their zeta potential values were monitored by laser Doppler microelectrophoresis at an angle of 22° using a Nano ZS90 Zetasizer (Malvern Instruments, United Kingdom). Transmission electron microscopy (TEM, JEM-2100F, JEOL, Japan) was used to observe the morphology of ECF after stained with 1% phosphotungstic acid. The absorption spectra of ECF were acquired using microplate spectrophotometer (Multiskan™ GO, Thermo Fisher Scientific, United States). Fluorescence spectrophotometer (F-4500, HITACHI, Japan) was used to record the emission spectra from 600 nm to 750 nm when excited at 400 nm. The content of Ce6 in ECF was calculated by its absorbance at 650 nm based on the established calibration curve (Figure S1). For the stability assay, CF and ECF were resuspended in PBS and 10% FBS-containing PBS at 4°C in the dark for 30 days. Changes in the hydrodynamic size and size distribution were monitored by DLS throughout the experiment.

SDS-PAGE was performed to confirm whether ECF possessed the similar membrane proteins from EM. ECF (10 μL, 10 mg mL^{-1} of nanoemulsion) was mixed with loading buffer (5 μL) under vortex at 100°C for 3 min. The resulting suspension was subsequently loaded and ran under electrophoresis at 120 V. After that, the protein bands were stained with coomassie brilliant blue and rinsed three times. The corresponding bare CF and EM were used as controls.[10]

Oxygen Loading and Releasing Profile of ECF

To investigate the oxygen-loading capacity, Ce6, CF, and ECF were individually added to deoxygenated PBS, and then saturated with oxygen for 30 min at room temperature. The oxygen concentration of each sample was evaluated using a portable dissolved oxygen meter (JPF-605B, REX, China) at oxygen equilibrium. For the assessment of oxygen-releasing behavior, preoxygenated nanoemulsion was added to deoxygenated PBS. The oxygen release behavior was recorded using an oxygen meter in real time. Meanwhile, the oxygen-releasing profile of preoxygenated PBS was used as a negative control.

Light-Triggered Singlet Oxygen Generation

1.3-diphenylisobenzofuran (DPBF), used as a molecular probe, was characterized by singlet oxygen ($^1O_2$) production of nanoemulsion.[28] The deoxygenated or preoxygenated Ce6, CF, and ECF (3 μg mL^{-1}, equivalent to Ce6) were added to the DPBF solution (100 μM in dimethyl formamide), which was then exposed to 660 nm laser (50 mW cm^{-2}, Rayan Tech., Changchun, China) for 3 min. The absorption spectra of each sample were recorded by a microplate spectrophotometer during the exposure period. Deoxygenated DW containing DPBF was set as a negative control.

Biocompatibility Test

The 3-(4,5-dimethylthiazol-2-yl)-2,5-diphenyltetrazolium bromide (MTT) assay was conducted to evaluate the cytotoxicity of ECF towards L929 or Raw 264.7 cells.[29] In short, the cells were seeded into a 96-well plate at a density of 2×10^4 cells per well. After 24 h of cell seeding, the cells were treated with serial concentrations of nanoemulsion for 12 h in the dark. Afterward, 20 μL of MTT (2.5 mg mL^{-1}) was added into each sample and incubated for another 4 h, and then their absorbance was measured at 570 nm via a microplate spectrophotometer. The PBS group was likewise subjected to the same procedure. All groups were assessed at least in sextuplicate.

The hemolytic behavior of ECF and CF was examined using mouse erythrocytes according to a standard protocol.[30] For that, erythrocytes were isolated and purified from whole blood by centrifugation (3000 × *g*, 15 min) and then diluted to 2% with normal saline. ECF or CF with different concentrations was added into diluted erythrocytes, which were incubated at 37°C for 1 h, respectively. After centrifugation at 3000 × *g* for 15 min, the absorbance of the supernatant was measured at 576 nm to determine the amount of hemoglobin released by the damaged erythrocytes. DW and normal saline were used as positive and negative control, respectively.

For evaluating the biocompatibility of nanoemulsion after illumination, the CF and ECF at serial concentrations were irradiated by 660 nm (50 mW cm^{-2}) for 3 min, respectively. The cells were similarly seeded into a 96-well plate and treated with light-irradiated nanoemulsion for 12 h in the dark. The cell viabilities were determined by MTT assay. Meanwhile, the diluted erythrocytes were incubated with light-irradiated nanoemulsion at 37°C for 1 h, and the hemolytic ratio of nanoemulsion was measured as described above.

Photodynamic Antibacterial Study

To investigate the photodynamic bactericidal ability of nanoemulsion, a standard plate counting method was carried out against *A. baumannii*.[12] Briefly, bacteria were cultured in Luria−Bertani broth medium at 37°C with shaking overnight and harvested during the exponential growth phase. After washing three times with cold PBS, the bacterial suspension was diluted to 10^8 CFU mL^{-1}. Subsequently, 900 μL bacterial suspension was incubated with Ce6, preoxygenated CF, and ECF at various concentrations (5, 10, 20, or 40 μg mL^{-1}, in terms of free Ce6) for 30 min at 37°C in dark, respectively. Following that, all samples were exposed to 660 nm light at an intensity of 100 mW cm^{-2} for 20 min. To evaluate the synergetic antibacterial efficiency of photodynamic and antibiotic therapy, preoxygenated ECF (10 μg mL^{-1}, in terms of free Ce6) and Gen at various concentrations (0.3, 0.5, 1, 2, or 4 μg mL^{-1}) were added

into the bacterial suspension. After incubation for 30 min, each sample was subjected to same irradiation process as above. The colony-forming units (CFU) were counted by inoculating 100 μL of diluted bacterial suspension onto LB agar plate and incubating 37°C for 24 h. PBS was set as a negative control. All experiments were performed independently in triplicate.

Macrophage Cell Uptake Study of ECF

To assess the potential of evading endothelial system clearance, the nanoemulsion was co-incubated with immune cells (Raw 264.7), and the cellular uptake behavior was examined via flow cytometry. Briefly, the cells were seeded at a density of 5×10^5 per well into a 24-well plate and cultured under the conditions of 5% CO_2 at 37°C. After 24 h of incubation, the cells were treated with PBS, Ce6, CF, or ECF (5 μg mL^{-1}, in terms of Ce6) for 2 h in the dark, respectively. Then, the cells were trypsinized and analyzed using a NovoCyte 2060R flow cytometer and ACEA NovoExpress software (ACEA Biosciences Inc., San Diego, Canada).

Pharmacokinetic Study

Male ICR mice (6–8 weeks) supplied by the Institute of Comparative Medicine of Yangzhou University were maintained in a pathogen-free environment (25 ± 2°C and 50 ± 5% humidity) under a 12 h light/dark cycle with free access to food and water. All animal experiments were approved by the Animal Care Committee of Nanjing Tech University (No. 20221111–01) prior to commencement. To evaluate the blood circulation profile of nanoemulsion, the mice (n = 3) were intravenously administered with Cy5.5-labeled CF or ECF at a dose of 3 mg kg^{-1} of liposome, respectively. Blood (approximately 10 μL) was collected from tail vein at predetermined time points post-administration, and the fluorescence intensity of blood sample was measured by the InVivo Smart-LF imaging system (Ex - 640 nm; Em - 740 nm, VIEWORKS Co., Republic of Korea). Moreover, non-compartmental pharmacokinetic parameters were calculated using the software program WinNonlin™ (Scientific Consulting Inc., United States). Meanwhile, the main pharmacokinetic parameters (MRT) were calculated using the non-compartmental method by dividing the total area under the curve (AUC).

Furthermore, the mice subjected to various treatments were maintained for an additional week. Afterward, the mice received the same treatment as described previously. The fluorescence intensity of blood sample was measured at the same time points, and then the non-compartmental pharmacokinetic parameters were calculated as described above.

In vivo Antibacterial Assay

Prior to the experiment, mice (No. 20240902–05) were intraperitoneally injected with cyclophosphamide (150 mg kg^{-1}) for 4 days to temporarily induce neutropenia. To establish an acute peritonitis infection model, the mice were treated with *A. baumannii* (1×10^7 CFU/20 g, 100 μL) via intraperitoneal injection. The mice were divided into five groups after being infected for 2 h: PBS, Gen, ECF+O_2+Gen, CF+O_2+Gen+Light and ECF+O_2+Gen+Light. The nanoemulsion (1 mg kg^{-1}, in terms of free Ce6) and Gen (50 μL, 1 mg mL^{-1}) were successively administrated via tail vein, and the infectious regions were exposed to 660 nm light irradiation (100 mW, 20 min) at 4 h post-treatment. Then the mice were euthanized and intraperitoneally injected with PBS (5 mL) to collect peritoneal fluid at 24 h post-treatment. Subsequently, the spleen, lung, and kidney were harvested and homogenized for 1 min. The bacteria in the peritoneal fluid and different organs were counted by the standard plate counting assay.

To investigate biosafety in vivo, mice (n = 3, No. 20240902–04) were treated with ECF+O_2 by intravenous injection. The control group was injected with PBS. At day 7 post-treatment, all mice were sacrificed to collect the primary organs (heart, liver, spleen, lung, and kidney), which were fixed with 4% paraformaldehyde, embedded in paraffin, sliced, stained with hematoxylin and eosin (H&E), and observed using an inverted optical microscope (Olympus, Japan).

Statistical Analysis

All statistical analyses were performed using GraphPad Prism (version 8.0, GraphPad Ltd., China). ANOVA was used to analyze all data with a Student-Newman-Keuls test for post-hoc pairwise comparisons.

Results and Discussion

Preparation of ECF

As shown in Figure 1A, CF was fabricated by ultrasonic emulsification and then wrapped with EM by self-assembly to form a long-circulating nanoemulsion (ECF). The average hydrodynamic size of CF and EM was 98.2 ± 5.1 nm and 137.5 ± 1.6 nm, respectively (Figure S2). When decorated with EM, the size of ECF increased to 110.9 ± 4.2 nm and its zeta potential was −13.6 ± 1.2 mV, which is similar to that of EM (−14.1 ± 0.8 mV, Figure 1B and S3). As revealed by the TEM images (Figure 1C and S4), CF and EM exhibited spherical morphology of approximately 100 nm each. Compared to CF, ECF displayed a spherical core-shell structure, possibly attributed to decoration with EM. Proteins on the membrane surface of erythrocyte which can provide several biological functions, such as long-term circulatory and immune escape capacity, play a vital role in various physiological processes.[22,23] SDS-PAGE analysis confirmed that the proteins preserved on ECF were comparable to those on the surface of EM; whereas no protein band was observed in CF as expected, implying successful modification of EM on the surface of nanoemulsion during the preparation process (Figure 1D). The UV-Vis spectra showed that CF and ECF featured characteristic absorption peaks of free Ce6 at 400 nm and 660 nm, while pure FDC exhibited no such characteristic absorption peak, indicating efficient loading of photoactive drug into nanoemulsion (Figure 1E). The loading capacity (LC) and encapsulation efficiency (EE) of drug were

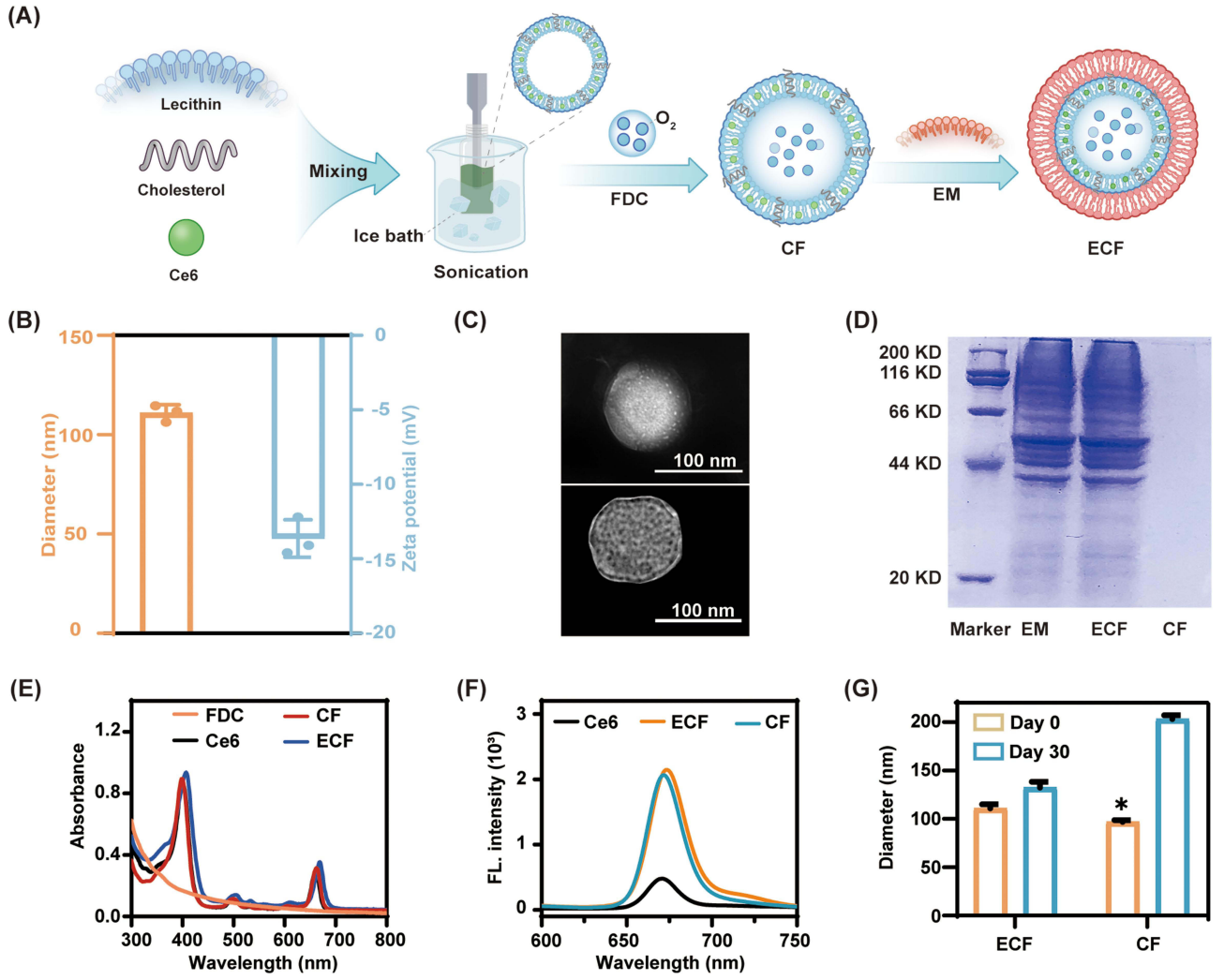

Figure 1 Characterizations of ECF. (**A**) Schematic diagram of the preparation of EM-coated CF (ECF). (**B**) Diameter and zeta potential of ECF. (**C**) Transmission electron microscopy (TEM) images of CF (top) and ECF (bottom). (**D**) The protein composition of ECF showed by SDS-PAGE analysis. The absorption (**E**) and emission (**F**) spectra of free Ce6, CF and ECF. (**G**) The stability of CF and ECF in PBS over 30 days. Data are shown as mean ± SD (n = 3). * $p < 0.005$, compared to the Day 30 group.

calculated to be 4.8% and 96.1%, respectively. With the severely limited solubility in aqueous conditions, free Ce6 emitted faint fluorescence when excited by 400 nm in DW. However, CF and ECF exhibited remarkable fluorescence emission at 673 nm, mainly because of the stabilizing ability of nanoemulsion towards the photoactive drug in aqueous environment (Figure 1F).

Furthermore, the colloidal stability of CF and ECF was preliminarily evaluated by monitoring the change of their hydrodynamic diameters. As shown in Figure 1G, the average size of CF notably increased from 97 to 203 nm in PBS at 4°C within 4 weeks. When resuspended in 10% FBS for a month, the size of CF increased by 140% compared to Day 0, showing a trend similar to that observed in PBS (Figure S5). This phenomenon is possibly due to the poor stability of naked nanoemulsion, which leads to accelerated swelling and aggregation of nanoemulsion under physiological condition or during long-term storage. In comparison, ECF displayed superior stability without significant change in size under identical experimental conditions, implying that enveloping with EM is a beneficial strategy for achieving a stable nanoemulsion. This may be partially explained that the dense polysaccharide on the surface of EM resembles a hydrophilic coating, which can improve the stability of nanoemulsion.[31] Based on these results, EM-encapsulated nanoemulsion loading photoactivity drug with excellent optical performance and good colloidal stability was successfully fabricated.

Oxygen Loading and Releasing Profile of ECF

Similar to hemoglobin-based materials, FDC possesses inherently strong oxygen loading potency.[14] Thus, introducing FDC into EM-decorated nanoemulsion could realize oxygen delivery and then oxygenation in local hypoxic infected-tissue. As depicted in Figure 2A, the oxygen content of CF+O_2 and ECF+O_2 was 15.6 ± 0.1 mg L^{-1} and 15.5 ± 0.2 mg L^{-1} at 2% v/v of FDC, respectively (Figure 2A) and their oxygen loading capacity is 2.3 folds than that of Ce6+O_2. These results demonstrated that wrapping with EM has scarcely impact on the oxygen-loading performance of nanoemulsion containing FDC. For exploring of oxygen releasing behavior, the preoxygenated nanoemulsion was added into deoxygenated DW, and the dissolved-oxygen concentration was monitored using a portable dissolved oxygen meter in real time. As expected, no obvious oxygen release behavior was observed in Ce6+O_2 group, which is in line with its poor oxygen-carrying ability. In contrast to the oxygen release profile of Ce6+O_2, the dissolved-oxygen concentration sharply increased after the addition of preoxygenated CF or ECF into deoxygenated water. The dissolved-oxygen concentration in CF+O_2 and ECF+O_2 group reached to 11.5 ± 0.2 mg mL^{-1} and 10.8 ± 0.5 mg mL^{-1}, respectively, within the first 30 min, and both of them maintained at a higher concentration (~15 mg mL^{-1}) even after 180 min (Figure 2B). Therefore, ECF showed remarkable oxygen loading potential and consistent oxygen releasing performance, which can serve as an excellent candidate for oxygen delivery for alleviating the local hypoxic conditions and enhancing the efficiency of PDT, in which oxygen is involved in $^1O_2$ production.

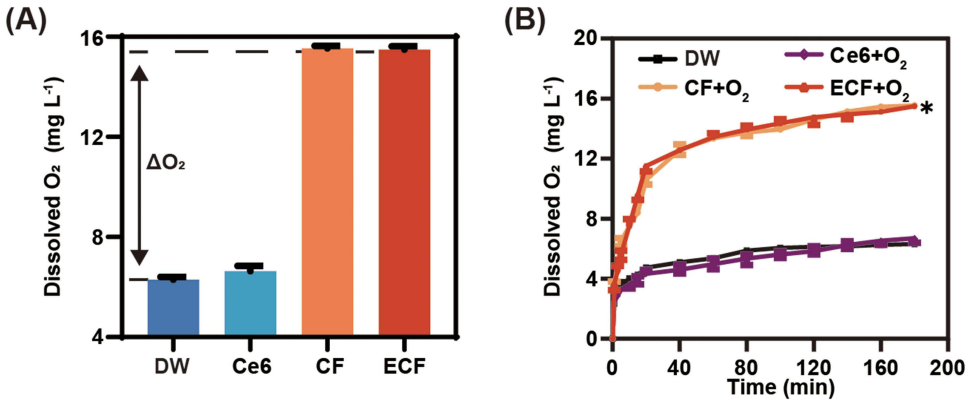

Figure 2 Oxygen loading and releasing behavior of ECF. (**A**) Dissolved oxygen concentration in DW after adding Ce6, CF and ECF, respectively. ΔO_2: enhanced O_2 concentration. (**B**) Dissolved oxygen concentration change after adding Ce6+O_2, CF+O_2 and ECF+O_2 in deoxygenated DW, respectively. Data are shown as mean ± S.D. ($n \geq 3$). * $p < 0.005$, compared to the Ce6+O_2 group.

Enhanced Photodynamic Activity

To assess the photodynamic performance of ECF in response to light irradiation, DPBF was used as a molecular probe to monitor singlet oxygen generation. As shown in Figure 3A–C, the absorbance of DPBF at 410 nm in Ce6+O_2 group sharply decayed compared with that in Ce6 group, which demonstrated that oxygen is an essential element in Ce6-mediated PDT. Moreover, we found that the DPBF-consuming rate in CF+O_2 and ECF+O_2 group closely resembled that in Ce6+O_2 group (Figure 3D and E). When irradiated with 660 nm for 180 s, the percentage of generated $^1O_2$ in CF+O_2 group and ECF+O_2 group rapidly rose to 72.9% and 81.8%, respectively (Figure 3F). However, marginal oxygen production was observed in the CF and ECF group under deoxygenated condition (Figure S6). Thus, FDC loaded into nanoemulsion with or without EM decoration would significantly reinforce the photodynamic activity of photosensitizers, particularly in hypoxic environments, which is in accordance with studies on oxygen-affording PDT.[14,30]

In vitro Biocompatibility Pattern

Before being applied to living systems, the biocompatibility of nanoemulsion should be clarified. To evaluate the cytotoxicity of ECF, L929 and Raw 264.7 were chosen to represent normal and immune cells, respectively. As shown in Figure 4A and B, neither CF nor ECF exhibited toxicity profiles regardless of cell type. After treatment for 12 h, the survival rate of cells subjected to CF or ECF treatment remained above 85%, even when their concentration reached 60 g mL^{-1} of liposome. After being exposed to 660 nm laser at an intensity of 100 mW cm^{-2} for 20 min, the nanoemulsion was then incubated with L929 and Raw 264.7 under identical experimental conditions. The viability of the cell following treatment with the nanoemulsion post-light irradiation remained ~90% (Figure S7). This funding indicated that CF and ECF are minimally toxic to mammalian cells. Furthermore, it is essential for nanoemulsions to be well tolerated by the host tissue without causing any undesirable effects, such as erythrocyte lysis.[32] When treated with CF or ECF, no obvious hemolysis was found in either CF or ECF group, and their hemolysis rate towards blood cells was lower than 5% at 60 μg mL^{-1} of liposome (Figure 4C and D). Moreover, the CF and ECF post-light irradiation have a negligible impact on blood cells, and their hemolysis rates are comparable to those of the nanoemulsion without illumination (Figure S8). Collectively, oxygen-affording nanoemulsion with or without EM modification has acceptable safety profiles in vitro, thereby widening the possibilities for further biomedical applications.

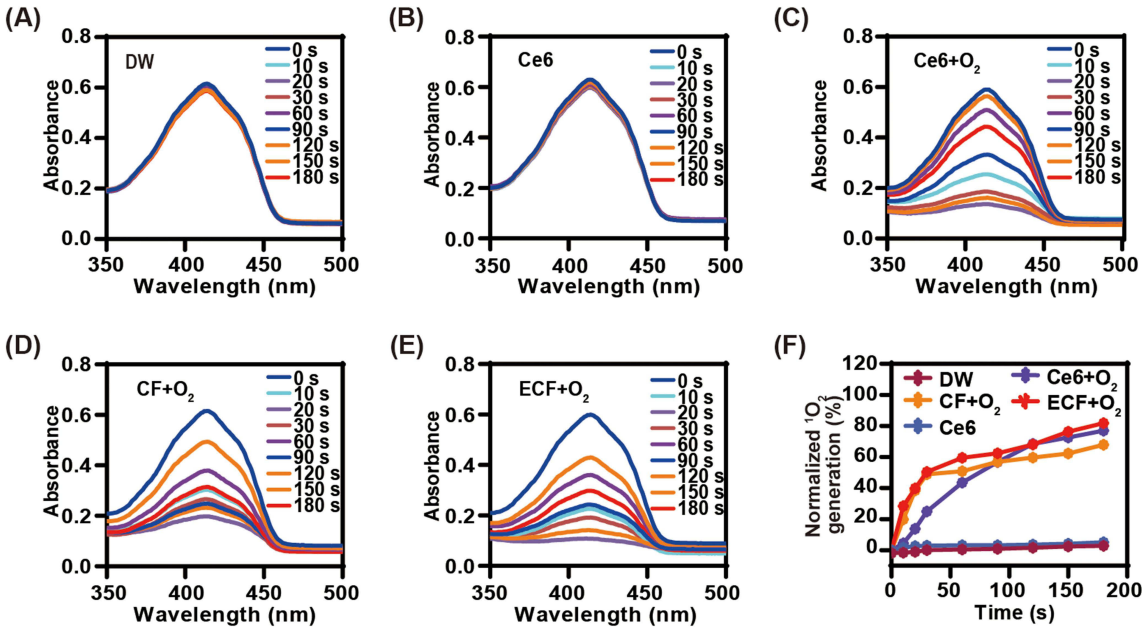

Figure 3 Singlet oxygen generation in response to light irradiation. Time-dependent absorption spectra of DPBF under 660 nm irradiation (50 mW cm^{-2}, 3 min) in the presence of DW (**A**), Ce6 (**B**), Ce6+O_2 (**C**), CF+O_2 (**D**) and ECF+O_2 (**E**), respectively. (**F**) Percentage of generated $^1O_2$ at predetermined time points in each group.

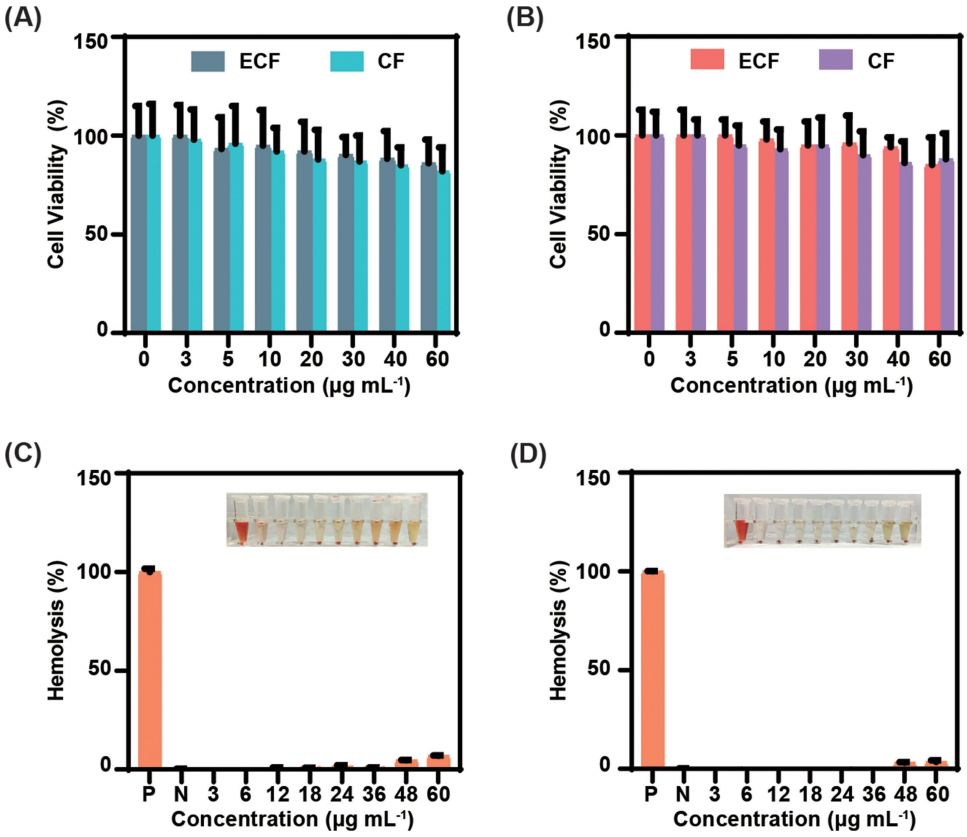

Figure 4 In vitro biocompatibility assay. Viability of L929 cells (**A**) and Raw264.7 cells (**B**) treated with CF and ECF at various concentrations. Hemolysis rates of RBC received CF (**C**) and ECF (**D**) treatment at 37 °C for 1 h. Inset showing the representative images of RBC with the corresponding treatments. (P) positive control, (N) negative control. Data are shown as mean ± S.D. (n ≥5).

Photodynamic Antibacterial Behavior

After demonstrating the photodynamic activity and biocompatibility of nanoemulsion, we then explored the bactericidal effect of preoxygenated ECF, which is a crucial therapeutic aspect for treating MDR Gram-negative bacterial infections. Figure 5A shows images of *A. baumannii* culture plates after various treatments. Numerous colonies were observed in Ce6 group plus light at 40 μg mL^{-1}, indicating the feeble bactericidal effect of Ce6. Because the cell envelope of Gram-negative bacteria is composed of an outer membrane, a thinner peptidoglycan layer, and a cytoplasmic membrane. The outer membrane which is rich in lipopolysaccharides prevents the uptake of anionic and neutral photosensitizers, leading to the refractory of gram-negative bacteria to PDT.[15] In contrast, the antibacterial performance of preoxygenated CF or ECF was greatly improved following light irradiation. We found that the bactericidal activity of Ce6, CF+O_2 and ECF+O_2 showed no obvious difference at 5 μg mL^{-1} of free Ce6, suggesting that nanoemulsion with EM coating could not alter the binding ability of nanoemulsion towards bacteria. While the viability of CF+O_2 and ECF+O_2 treated bacteria reduced to 2.6% and 2.0%, respectively, at 40 μg mL^{-1} of free Ce6, displaying augment photodynamic bactericidal effect against MDR Gram-negative bacteria (Figure 5B). We hypothesized that continuous oxygen supplement and high dose PS can rapidly generate large amounts of ROS during light irradiation. This process is advantageous for disrupting the structure of membrane through the oxidation of biomolecules, ultimately resulting in bacterial lysis. This result verified that gram-negative bacteria treated with oxygen-loaded nanoemulsion were sensitized to PDT, which is consistent with our previous study.[14] Furthermore, we found that the bacterial survival rate prominently decreased, accompanied by increasing the concentration of photosensitive drug in CF+O_2 and ECF+O_2 group plus illumination, indicating a dose-dependent manner. In addition, CF+O_2 and ECF+O_2 displayed similar bactericidal activities at concentrations between 0 and 40 μg mL^{-1}, suggesting that wrapping with EM barely affected the bactericidal activity of oxygen-affording

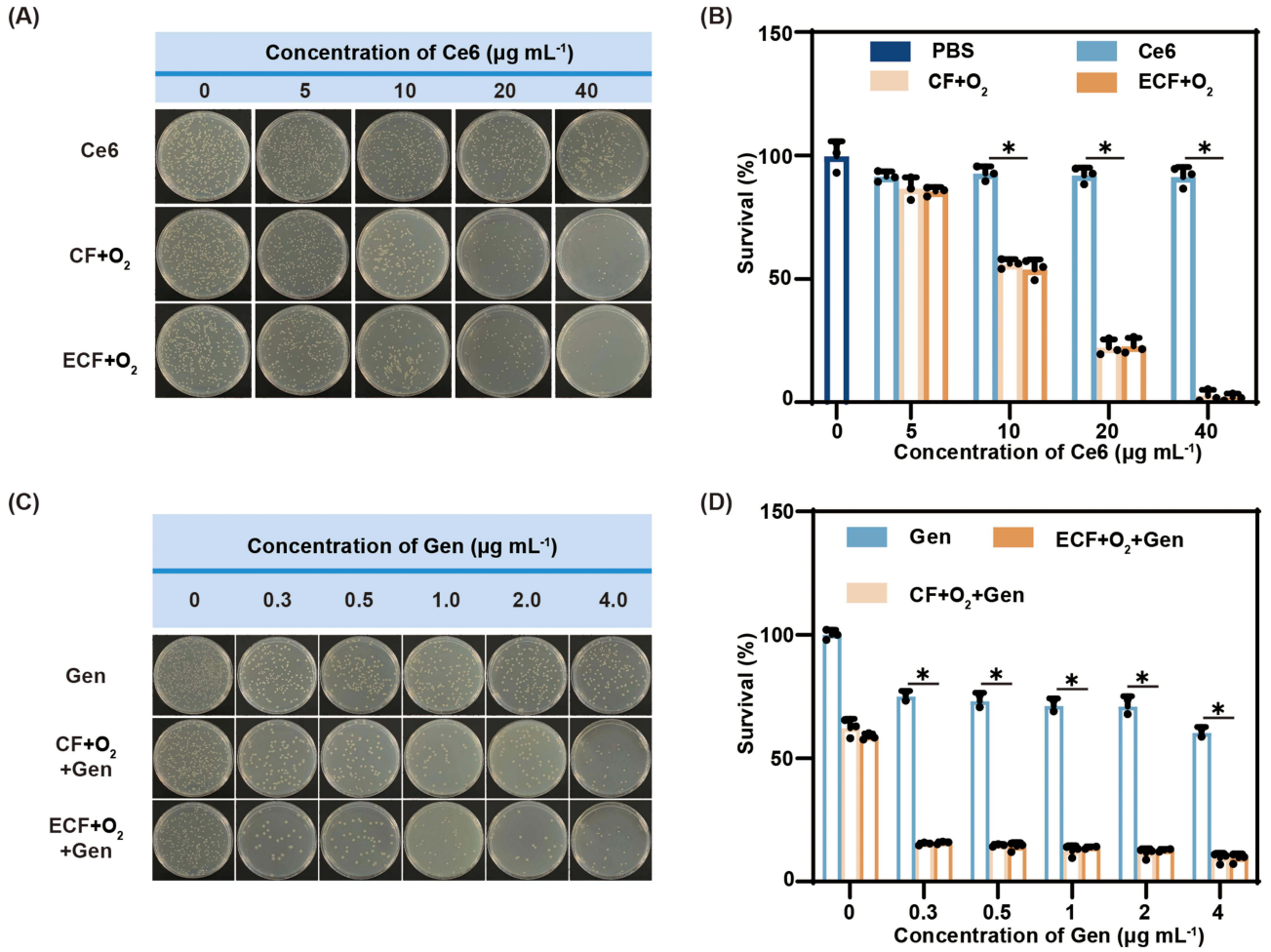

Figure 5 In vitro synergistic bactericidal performance of combining ECF+O_2 and antibiotics against multidrug-resistant Gram-negative bacteria. Representative images (**A**) and survival rate (**B**) of *A. baumannii* received Ce6, CF+O_2 or ECF+O_2 treatment under light irradiation (660 nm, 100 mW cm^{-2}, 20 min). Representative images (**C**) and survival rate (**D**) of *A. baumannii* treated with Gen, CF+O_2+Gen or ECF+O_2+Gen at various concentrations in dark or under illumination as described above. Data are shown as mean ± S.D. (n ≥ 3). * $p < 0.005$.

nanoemulsion. Therefore, the oxygen supply may sensitize MDR Gram-negative bacteria towards PDT and trigger conspicuous antibacterial potency as irradiation proceeded.

Furthermore, we explored the synergistic bactericidal behavior of oxygen-affording nanoemulsion and antibiotic against *A. baumannii* over irradiation course. As depicted in Figure 5C, the number of viable bacteria showed marginal reduction when incubated with Gen in the dark and more than 60% of the bacteria survived at 4.0 μg mL^{-1}, displaying poor antibacterial potency of Gen towards *A. baumannii*. These phenomena again demonstrated that *A. baumannii* is easily resistant to antibiotics, causing repetitive bacterial infections during the treatment period.[33] Compared with antibiotic therapy alone, the viability of bacteria treated with oxygen-affording nanoemulsion and antibiotic rapidly decreased in response to light irradiation. When exposed to illumination for 20 min, the bactericidal rate in preoxygenated ECF+Gen group reached to 84.5% at 0.3 μg mL^{-1} of Gen, which is 3.3–fold higher than that in the Gen group, exhibiting notable bactericidal effect. Meanwhile, the combination of preoxygenated CF and Gen also showed an analogous bacterial killing performance under identical experimental conditions (Figure 5D). Because the large amount of ROS generated by CF or ECF in response to illumination could damage biomolecules, such as lipids and proteins of membrane, leading to destabilization of the bacterial structure. This, in turn, accelerated the internalization of gentamicin, which inhibits bacterial protein synthesis, thereby amplifying synergistic bactericidal efficiency. Collectively, these results provided a novel strategy to combat MDR Gram-negative bacterial infectious diseases by combining oxygen-containing PDT with antibiotic therapy.

Immune Evasion Capacity in vitro

Encouraged by the superior antibacterial performance of the preoxygenated ECF against MDR gram-negative bacteria, we then investigated the "stealthy potential" of ECF towards immune cells in vitro. Following the incubation with Raw 264.7 for 2 h, it was noted that Ce6 and CF were promptly internalized by cells. This phenomenon may be ascribed to the rapid recognition and capture of nanoemulsion by immune cells based on the inherent characteristics of exogenous materials (Figure 6A). However, in the presence of EM-enveloping, ECF displayed a notable antiphagocytosis effect under identical experimental conditions, which was superior to that of either Ce6 or CF. Quantitative analysis revealed that the antiphagocytosis rate in ECF group was 100% higher than that in CF group (Figure 6B). The underlying mechanism of such antiphagocytosis profile is possible because there are numerous "self-recognition" proteins (such as CD47) on the surface of EM, which release 'don't eat-me' signal to evade uptake by immune cells.[24,25] These results suggested that modifying oxygen-affording nanoemulsion with EM empowers the immune-escape potential, which is beneficial for prolonging the half-life of drug and enhancing therapeutic efficacy in vivo.

Pharmacokinetics in vivo

Motivated by the desirable immune escape behavior of ECF in vitro, pharmacokinetic behaviors in vivo were evaluated following intravenous administration of Cy5.5-labeled nanoemulsion, and then the photon counts in sampled blood were analyzed at indicated time points. As shown in Figure 7A, the ECF level in the bloodstream was 19-fold higher than the CF level at 48 h post-administration. Compared to CF, the AUC of ECF increased by 35% (19,935,509 ± 1455307

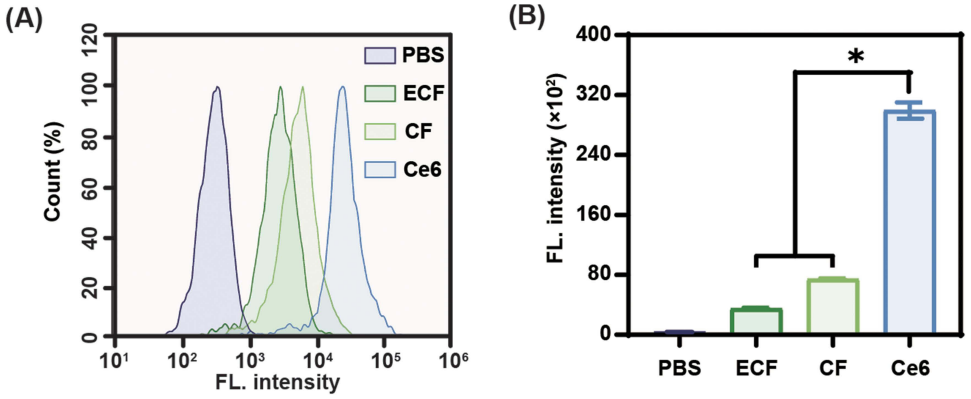

Figure 6 In vitro immune-escape profile of ECF. (**A**) Flow cytometry analysis of Raw 264.7 cells incubated with Ce6, CF or ECF (5 μg mL^{-1}, in terms of Ce6) for 2 h in dark. (**B**) Quantitative analysis of fluorescence intensity based on (**A**). Data are shown as mean ± S.D. (n ≥ 3). * p < 0.005.

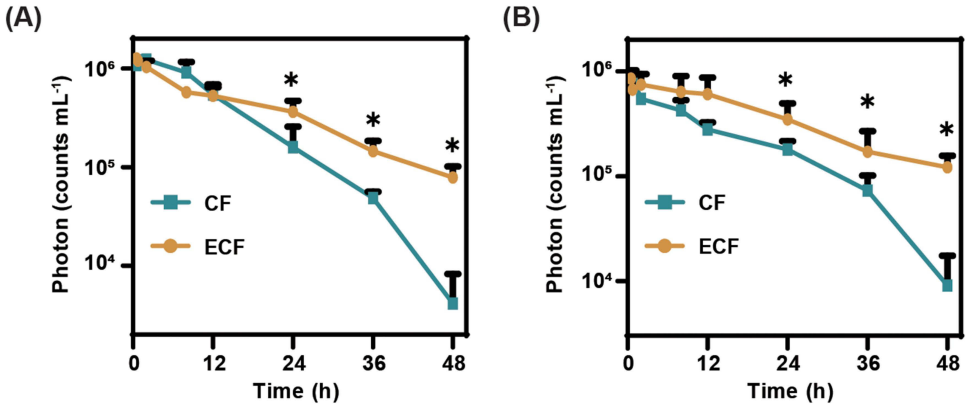

Figure 7 Blood concentration-time curve after intravenous administration of CF or ECF. (**A**) Mice were intravenously injected with Cy5.5-labeled CF or ECF and then their blood was collected for fluorescence intensity measurement at predetermined time points over the subsequent 48 h. (**B**) Mice received same treatment at day 9 after first administration and their fluorescence intensity of blood sample was acquired as above. Data are shown as mean ± S.D. (n ≥ 3). *p < 0.005, compared to the CF group.

photon counts/mL·h for ECF versus 15505344 ± 2946157 photon counts/mL·h for CF). Moreover, the MRT of the ECF was 14.5 ± 0.7 h, which was 1.5-fold than that of CF (Table S1). Inheriting the immune-evading potential of "mother cells", ECF exhibited lower reticuloendothelial system clearance and extended systemic circulation of the drug in vivo.

Polyethylene glycol (PEG) modification is commonly introduced into various nanoplatforms to improve their stability and promote drug retention in the blood. Unfortunately, the production of antibodies against PEG accelerated the clearance of drugs from the blood (ABC phenomenon) when immune cells were exposed to the second stimulus of PEG.[34] Therefore, it is necessary to explore the pharmacokinetic patterns following the second administration. For that, the mice received the same treatment at day 9 after the initial administration and their pharmacokinetic profiles were acquired as described above. The ECF level in the blood was higher than the CF level over 48 h post-treatment (Figure 7B). ECF also exhibited a prolonged half-life (12.4 ± 1.1 h) and larger MRT (15.1 ± 1.2 h) in the blood, which was similar to that of the first administration (Table S1). Based on these results, ECF showed long-term circulation in vivo, promoting accumulation of drug at infectious site.

Therapeutic Effect in vivo

To investigate the therapeutic effects of oxygen-affording nanoemulsion in vivo, a systemic infection model of *A. baumannii*-induced acute peritonitis was established in mice (Figure 8A). The infected mice were treated with PBS, Gen, preoxygenated CF+Gen and preoxygenated ECF+Gen plus light or not. As shown in Figure 8B, the number of survived bacteria in the peritoneal fluid of infected mice subjected to Gen, ECF+O_2+Gen and CF+O_2+Gen+Light treatments partially decreased compared to the infected mice in the PBS group. The poor bactericidal performance observed in Gen, ECF+O_2+Gen and CF+O_2+Gen+Light groups suggested that neither antibiotic therapy nor photodynamic therapy alone could achieve a better therapeutic effect in fighting against gram-negative bacterial infections. In contrast, the log values of CFU, where it dropped to 3.6 ± 0.2 for ECF+O_2+Gen+Light group, approximately 3.0 log units lower than that in the Gen group, demonstrating enhanced antibacterial potency. Moreover, the number of viable bacteria in the lung, spleen, and kidney in ECF+O_2+Gen+Light group was notably lower than in the other groups, showing great potential for the treatment of peritonitis-induced systemic infections. In addition, histological analysis of the major organs (heart, liver, spleen, lung, and kidney) of mice received ECF+O_2 treatment presents an integrated tissue

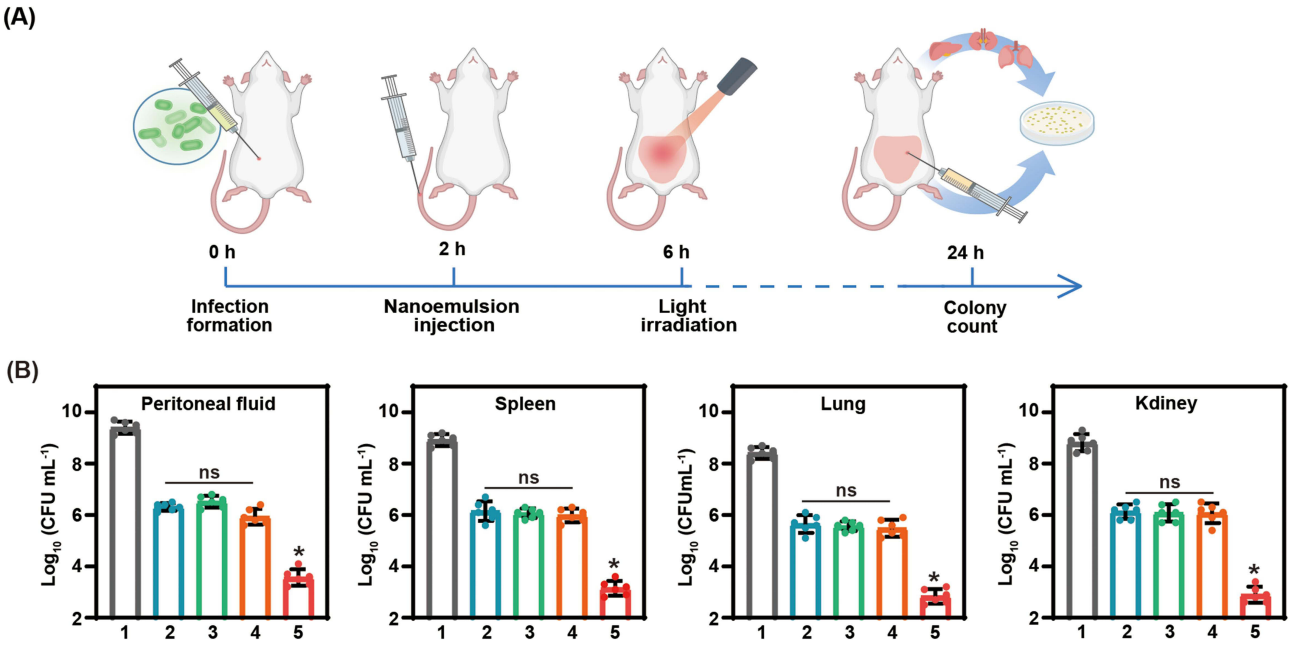

Figure 8 Light-triggered therapeutic effects of ECF+O_2 against bacterial infection in vivo. (**A**) Schematics of the experiments to evaluate the therapeutic efficacy of Gen+ECF+O_2 plus light irradiation in combating *A. baumannii*–induced acute peritonitis. (**B**) Quantification of the number of bacteria in peritoneal fluid, spleen, lung and kidney of the infected mice received various treatments (1: PBS; 2: Gen, 1 mg mL^{-1} of Gen; 3 ECF+O_2+Gen, 1 mg kg^{-1} of Ce6; 4: CF+O_2+Gen +Light; 5: ECF+O_2+Gen +Light). Data are shown as mean ± S.D. (n ≥ 6). ns: no significant difference, *p < 0.005, compared to the Gen+CF+O_2+Light group.

structure without any abnormal defects or damage (Figure S9), indicating that the ECF+O_2 can serve as a safe therapeutic nanoemulsion for combating *A. baumannii*-induced acute peritonitis.

Conclusion

In summary, erythrocyte membrane-cloaked nanoemulsion co-loading photosensitive drug and oxygen (ECF) with excellent optical activity, good colloidal stability and "stealthy potential" was successfully constructed. It exhibits acceptable cytocompatibility to tissue cells, as well as hemocompatibility. In vitro studies demonstrated that ECF has a superior potential for oxygen loading and release, light-triggered singlet oxygen generation, and escape immune cell uptake. We also proved the effectiveness of ECF in sensitizing *A. baumannii* to PDT, resulting in enhanced bactericidal performance via the combination of oxygen-affording PDT and antibiotic therapy. Furthermore, ECF exhibited lower reticuloendothelial system clearance, prolonged blood retention in vivo, and enhanced therapeutic efficacy against *A. baumannii*-induced acute peritonitis in mice. Collectively, it is believed that our ECF, with its inherent antiphagocytosis, long circulation, co-delivery of oxygen and photosensitizer ability and capacity to sensitize and eliminate gram-negative bacteria, represents a promising candidate for an integrated nanoplatform aimed at combating MDR Gram-negative bacterial infections.

Abbreviations

PDT, photodynamic therapy; MDR, multidrug-resistant; FDC, perfluorocarbon; Ce6, Chlorin e6; Gen, gentamicin; *A. baumannii, Acinetobacter baumannii*; PS, photosensitizers; ROS, reactive oxygen species; RES, reticuloendothelial system; MPS, mononuclear phagocyte system; SIRPα, signal-regulatory protein alpha; EM, erythrocyte membrane; DPBF, 1.3-diphenylisobenzofuran; BCA, Bicinchoninic acid; SDS-PAGE, sodium dodecyl sulfate-polyacrylamide gel electrophoresis; DW, distilled water; Raw 264.7, Mouse macrophages cell; L929, fibroblasts cell; Ce6, Ce6 nanoemulsion; CF, Ce6@FDC nanoemulsion; ECF, EM-coated CF nanoemulsion; DLS, dynamic light scattering; TEM, transmission electron microscopy; $^1O_2$, singlet oxygen; MTT, 3-(4,5-dimethylthiazol-2-yl)-2,5-diphenyltetrazolium bromide; CFU, colony-forming units; MRT, the main pharmacokinetic parameters; AUC, the total area under the curve; PEG, Polyethylene glycol.

Acknowledgments

This work was supported by research grants from the National Natural Science Foundation of China (No. 51603101), the National Natural Science Foundation of China (No. 22408076), the Natural Science Foundation of Jiangsu Higher Education Institutes of China (No. 22KJB530006), the Hainan Provincial Natural Science Foundation of China (No. 824QN267) and The Open Foundation of NHC Key Laboratory of Tropical Diseases Control, Hainan Medical University (No. 2023NHCTDCKFKT21003).

Disclosure

The authors declare that they have no known competing financial interests or personal relationships that could have appeared to influence the work reported in this study.

References

1. Cars O, Chandy SJ, Mpundu M, et al. Resetting the agenda for antibiotic resistance through a health systems perspective. *Lancet Glob Health*. 2021;9(7):e1022–e1027. doi:10.1016/S2214-109X(21)00163-7
2. Akeda Y. Current situation of carbapenem-resistant *Enterobacteriaceae* and *Acinetobacter* in Japan and Southeast Asia. *Microbiol Immunol*. 2021;65(6):229–237. doi:10.1111/1348-0421.12887
3. Wang H, Yang Y, Wang S, et al. Antimicrobial sensitisers: gatekeepers to avoid the development of multidrug-resistant bacteria. *J Control Release*. 2024;369:25–38. doi:10.1016/j.jconrel.2024.03.031
4. Sherif E, Ahmed ME, Mohamed AE, et al. Enhanced photocatalytic and antibacterial activities of novel Ag-HA bioceramic nanocatalyst for waste-water treatment. *Sci Rep*. 2023;13(1):13819. doi:10.1038/s41598-023-40970-4
5. Ahmed ME, Mohamed A, Hafez O, et al. Photocatalytic, antimicrobial and antibiofilm activities of $MgFe_2O_4$ magnetic nanoparticles. *Sci Rep*. 2024;14(1):12877. doi:10.1038/s41598-024-62868-5

6. Ahmed IE, Nawal EA, Ayman AF, et al. Antimicrobial synergism and antibiofilm activity of amoxicillin loaded citric acid-magnesium ferrite nanocomposite: effect of UV-illumination, and membrane leakage reaction mechanism. *Microb Pathogenesis*. 2022;164:105440. doi:10.1016/j.micpath.2022.105440
7. Geng ZM, Cao ZP, Liu JY, et al. Recent advances in targeted antibacterial therapy basing on nanomaterials. *Exploration*. 2023:20210117. doi:10.1002/EXP.20210117
8. Kwon JH, Powderly WG. The post-antibiotic era is here. *Science*. 2021;373(6554):471. doi:10.1126/science.abl5997
9. Uddin TM, Chakraborty AJ, Khusro A, et al. Antibiotic resistance in microbes: history, mechanisms, therapeutic strategies and future prospects. *J Infect Public Health*. 2021;14(12):1750–1766. doi:10.1016/j.jiph.2021.10.020
10. Feng Y, Coradi Tonon C, Ashraf S, et al. Photodynamic and antibiotic therapy in combination against bacterial infections: efficacy, determinants, mechanisms, and future perspectives. *Adv Drug Deliv Rev*. 2021;177:113941. doi:10.1016/j.addr.2021.113941
11. Sun Y, Sun X, Li X, et al. A versatile nanocomposite based on nanoceria for antibacterial enhancement and protection from aPDT-aggravated inflammation via modulation of macrophage polarization. *Biomaterials*. 2021;268:120614. doi:10.1016/j.biomaterials.2020.120614
12. Jin Y, Wang C, Xia Z, et al. Photodynamic chitosan sponges with dual instant and enduring bactericidal potency for treating skin abscesses. *Carbohydr Polym*. 2023;306:120589. doi:10.1016/j.carbpol.2023.120589
13. Zou L, Hu D, Wang F, et al. The relief of hypoxic microenvironment using an O_2 self-sufficient fluorinated nanoplatform for enhanced photodynamic eradication of bacterial biofilms. *Nano Res*. 2022;15(2):1636–1644. doi:10.1007/s12274-021-3712-5
14. Niu P, Dai J, Wang Z, et al. Sensitization of antibiotic-resistant Gram-negative bacteria to photodynamic therapy via perfluorocarbon nanoemulsion. *Pharmaceuticals*. 2022;15:156. doi:10.3390/ph15020156
15. Hu D, Zou L, Yu W, et al. Relief of biofilm hypoxia using an oxygen nanocarrier: a new paradigm for enhanced antibiotic therapy. *Adv Sci*. 2020;7(12):2000398. doi:10.1002/advs.202000398
16. Li X, Kwon N, Guo T, et al. Innovative strategies for hypoxic-tumor photodynamic therapy. *Angew Chem Int Ed Engl*. 2018;57(36):11522–11531. doi:10.1002/anie.201805138
17. Wu B, Sun Z, Wu J, et al. Nanoparticle-stabilized oxygen microcapsules prepared by interfacial polymerization for enhanced oxygen delivery. *Angew Chem Int Ed Engl*. 2021;60(17):9284–9289. doi:10.1002/anie.202100752
18. Che J, Sun L, Shan J, et al. Artificial lipids and macrophage membranes coassembled biomimetic nanovesicles for antibacterial treatment. *Small*. 2022;18(26):2201280. doi:10.1002/smll.202201280
19. Shi R, Lv R, Dong Z, et al. Magnetically-targetable outer-membrane vesicles for sonodynamic eradication of antibiotic-tolerant bacteria in bacterial meningitis. *Biomaterials*. 2023;302:122320. doi:10.1016/j.biomaterials.2023.122320
20. Nguyen PHD, Jayasinghe MK, Le AH, et al. Advances in drug delivery systems based on red blood cells and their membrane-derived nanoparticles. *ACS Nano*. 2023;17(6):5187–5210. doi:10.1021/acsnano.2c11965
21. Xia Q, Zhang Y, Li Z, et al. Red blood cell membrane-camouflaged nanoparticles: a novel drug delivery system for antitumor application. *Acta Pharm Sin B*. 2019;9(4):675–689. doi:10.1016/j.apsb.2019.01.011
22. Zhang W, Zhao M, Gao Y, et al. Biomimetic erythrocytes engineered drug delivery for cancer therapy. *Chem Eng J*. 2022;433:133498. doi:10.1016/j.cej.2021.133498
23. Glassman PM, Hood ED, Ferguson LT, et al. Red blood cells: the metamorphosis of a neglected carrier into the natural mothership for artificial nanocarriers. *Adv Drug Deliv Rev*. 2021;178:113992. doi:10.1016/j.addr.2021.113992
24. Ran L, Lu B, Qiu H, et al. Erythrocyte membrane-camouflaged nanoworms with on-demand antibiotic release for eradicating biofilms using near-infrared irradiation. *Bioact Mater*. 2021;6(9):2956–2968. doi:10.1016/j.bioactmat.2021.01.032
25. Chen Y, Li Y, Liu J, et al. Erythrocyte membrane bioengineered nanoprobes via indocyanine green-directed assembly for single NIR laser-induced efficient photodynamic/photothermal theranostics. *J Control Release*. 2021;335:345–358. doi:10.1016/j.jconrel.2021.05.025
26. Liu W, Ruan M, Wang Y, et al. Light-triggered biomimetic nanoerythrocyte for tumor-targeted lung metastatic combination therapy of malignant melanoma. *Small*. 2018;14(38):1801754. doi:10.1002/smll.201801754
27. Li Y, Xiong J, Hu Y, et al. Wrapping collagen-based nanoparticle with macrophage membrane for treating multidrug-resistant bacterial infection. *J Leather Sci Eng*. 2022;4(1):31. doi:10.1186/s42825-022-00106-2
28. Li Y, Feng P, Wang C, et al. Black phosphorus nanophototherapeutics with enhanced stability and safety for breast cancer treatment. *Chem Eng J*. 2020;400:125851. doi:10.1016/j.cej.2020.125851
29. Li Y, Xiong J, Guo W, et al. Decomposable black phosphorus nano-assembly for controlled delivery of cisplatin and inhibition of breast cancer metastasis. *J Control Release*. 2021;335:59–74. doi:10.1016/j.jconrel.2021.05.013
30. He X, Guo W, Tang Y, et al. Chloroplast–boosted photodynamic therapy for effective drug-resistant bacteria killing and biofilm ablation. *J Photochem Photobiol B*. 2023;238:112622. doi:10.1016/j.jphotobiol.2022.112622
31. Kroll AV, Fang RH, Zhang L. Biointerfacing and applications of cell membrane-coated nanoparticles. *Bioconjug Chem*. 2017;28(1):23–32. doi:10.1021/acs.bioconjchem.6b00569
32. Li Y, Li X, Yu J, et al. A versatile diketopyrrolopyrrole-based photosensitizing nanoplatform with high photostability and photoactivity for metastatic breast cancer treatment. *Dyes Pigm*. 2022;207:110748. doi:10.1016/j.dyepig.2022.110748
33. Ren HM, Han L, Zhang L, et al. Inhalable responsive polysaccharide-based antibiotic delivery nanoparticles to overcome mucus barrier for lung infection treatment. *Nano Today*. 2022;44:101489. doi:10.1016/j.nantod.2022.101489
34. Knop K, Hoogenboom R, Fischer D, et al. Poly(ethylene glycol) in drug delivery: pros and cons as well as potential alternatives. *Angew Chem Int Ed Engl*. 2010;49(36):6288–6308. doi:10.1002/anie.200902672